Seasonal Variations of Solar Wind Parameters during Solar Cycles 23 and 24

Somaïla Koala[1], Yacouba Sawadogo[1], Jean Louis Zerbo[1,2*]

[1]Laboratoire de Matériaux, d'Héliophysique et Environnement (La.M.H.E), ED/ST, Université Nazi BONI, Bobo-Dioulasso, Burkina Faso
[2]Unité de Formation et de Recherche en Sciences Exactes et Appliquées (UFR/SEA), Université Nazi BONI, Bobo-Dioulasso, Burkina Faso
Email: *jeanlouis.zerbo@gmail.com

Abstract

In this paper, we analyzed diurnal and annual seasonal variations of solar wind parameters such as interplanetary magnetic field (IMF), proton density (N), solar wind speed (V) and solar wind dynamic pressure (Pdym), during the solar cycles 23 and 24. Our study shows that strong geomagnetic disturbances are observed at the equinoxes during both solar cycles. The highest proton densities are observed at solstices during both solar cycles. The greatest solar wind speeds are observed at the equinoxes of solar cycle 23 and at the solstices of solar cycle 24. The highest solar wind dynamic pressures are observed at the solstices of both solar cycles. We also observed an asymmetrical evolution of the seasonal diurnal values of the solar wind parameters during the two cycles, except for the proton density. Our investigations also highlight the fact that the seasonal diurnal values of the solar wind parameters are significant at solar cycle 23 compared to solar cycle 24 characterized by a global weak in solar plasma conditions since the deep minimum that followed the solar cycle 23 leading to an absence of a persistent polar coronal hole. The drop observed in polar field and solar winds parameters during solar cycle 24 is reproduced on seasons (solstices and equinoxes). The solar cycle 23 and 24 appear to be two magnetically opposite solar cycles regardless the time scales.

Keywords

Diurnal, Seasonal, Solar Winds, Parameters, Variation, Solar Cycle

1. Introduction

The solar wind is a stream of charged particles released from the upper atmos-

phere of Sun, called the corona. It provides a highly variable source of energy to the interplanetary medium. The large-scale evolution of the solar wind is determined by the solar magnetic field whose structure varies during the solar cycle [1] [2] [3]. The solar magnetic field carried outward by the solar wind in the heliosphere when the magnetic field lines of the Sun are driven by the highly conductive solar wind plasma is called the interplanetary magnetic field (IMF) [4]. The dynamics of this wind is responsible for 91.5% of geomagnetic activity [5] [6] [7]. The solar wind and the magnetosphere constantly interact, thus constituting a coupled system, because the disturbances of the interplanetary medium cause geomagnetic disturbances [8]. According to [9] [10] coronal mass ejections and co-rotating interaction regions/high-velocity fluxes striking the Earth's magnetic field are the main drivers of geomagnetic activity. Coronal mass ejections produce the majority of strong geomagnetic storms, and co-rotating/high-velocity flux interaction regions produce a large proportion of minor to moderate intensity storms. The highest solar wind speeds are observed during the descending phase of the solar cycle, when high-velocity flows from equator ward extensions of polar coronal holes often reach low heliographic latitudes and the ecliptic plane [5] [11] [12]. Annual averages of solar wind speed provide important insight into the long-term evolution of solar magnetic fields and coronal holes, but a study using higher temporal resolution is useful because the typical lifetime of coronal holes is several solar rotations but less than a year [13] [14] [15] [16]. So deep investigation on solar plasma becomes of great interest to better understand the behavior of solar wind. Our present work aims to analyze the seasonal diurnal variation of solar wind parameters during the solar cycles 23 and 24. Our work will be structured as follows: Section 2 is devoted to methodology and data processing; Section 3 to the results and discussion and in Section 4 we summary our findings.

2. Data and Methodology

In this study, we study the variations of the solar wind parameters such as the interplanetary magnetic field, the proton density, the solar wind speed and the dynamic pressure of the solar wind according to the solar cycle, the season and the day. To achieve our objective, we used the hourly values of these parameters, available on the site https://omniweb.gsfc.nasa.gov/form/dx1.html. The arithmetic mean values calculated from the hourly values of the parameters are used to study the diurnal variation. The seasonal variation and the annual variation are obtained by using the arithmetic mean values of the monthly and annual values respectively. The seasons are distributed as follows: Winter (December, January and February), spring (March, April and May), summer (June, July, and August), autumn (September, October and November).

To calculate the relative difference or relative deviation of the months of equinoxes and solstices of the solar wind parameters, we used the following formula.

For IMF, we have:

$$\Delta IMF_{-Solstice} = \frac{IMF_{summer} - IMF_{winter}}{IMF_{summer}} \times 100 \qquad (1)$$

$$\Delta IMF_{-Equinox} = \frac{IMF_{spring} - IMF_{autumn}}{IMF_{spring}} \times 100 \qquad (2)$$

$\Delta IMF_{-Solstice} > 0$ (<0): Summer measurement is greater (smaller) than that of winter.

$\Delta IMF_{-Equinox} > 00$ (<0): Spring measurement is greater (smaller) than that of autumn.

For the other parameters, only replace IMF by the corresponding parameters.

3. Results and Discussions

3.1. Diurnal Seasonal Variations

Figure 1(a), presents the diurnal seasonal variation of IMF during solar cycle 23. This figure shows that, the highest diurnal values of IMF during solar cycle 23
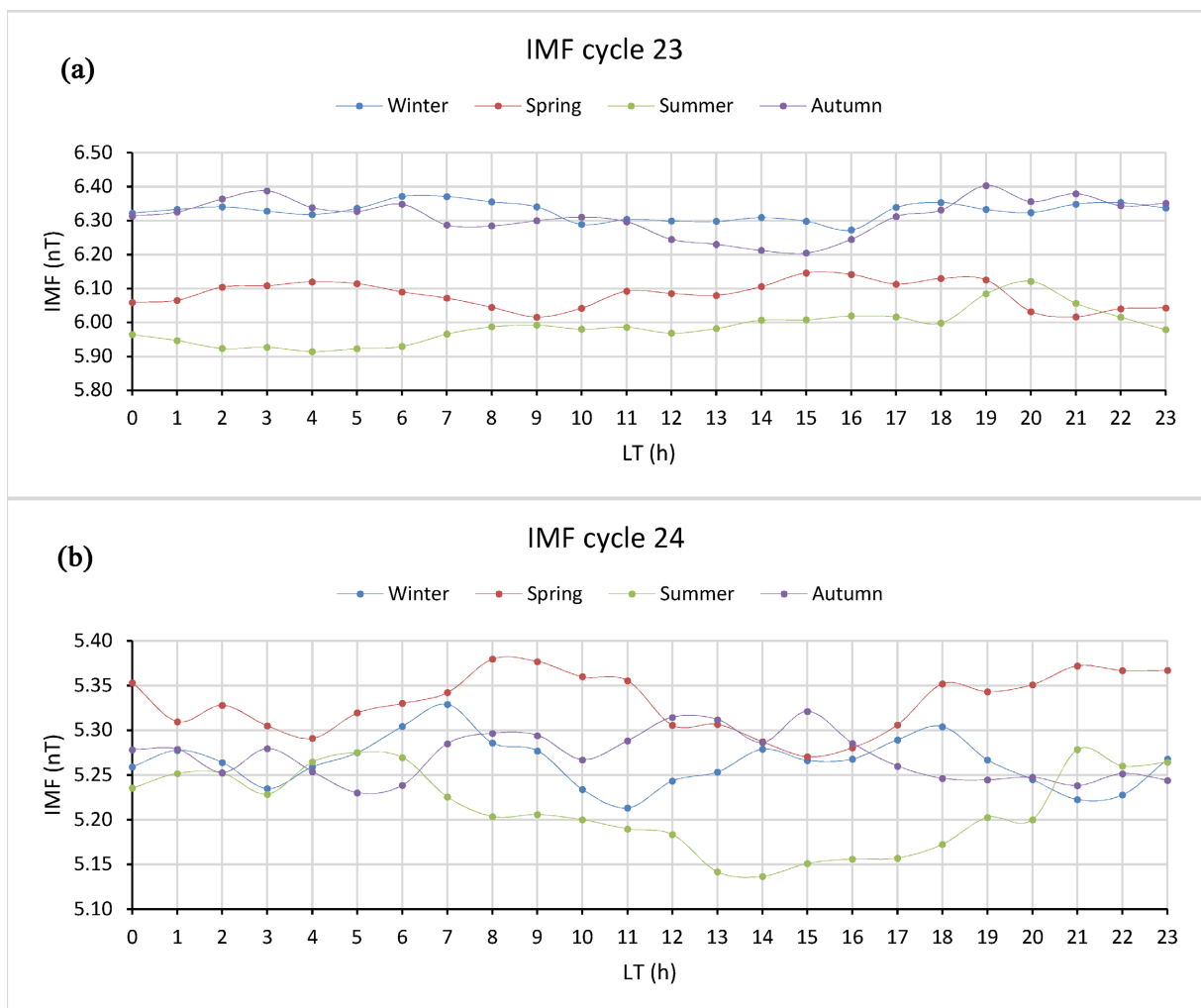
Figure 1. Seasonal diurnal variation of IMF during solar cycle 23 (a) and solar cycle 24 (b).

are generally observed during autumn and a few times during the winter between 06:00 LT and 09:00 LT; then between 12 h and 18:00 LT. The lowest diurnal values of the IMF are recorded during the summer except after 19 h and just before 22h. The lowest diurnal values of the IMF are recorded during the summer. We observe a weak fluctuation of the IMF during the four seasons during cycle 23. The equinoxes (spring and autumn) and the solstices (winter and summer) are asymmetrical during cycle 23; the values of IMF in autumn are higher than those in spring (**Figure 1(b)**) and the values of IMF in winter are higher than those in summer (**Figure 1(a)**).

Figure 1(b) presents the seasonal diurnal variation of the IMF during solar cycle 24. This figure shows that the highest diurnal values of the IMF during solar cycle 24 are observed during spring except on the times intervals [12:00 LT-13: 00 LT] and [14:00 LT-16: 00 LT] where highest values are recorded during autumn. The lowest diurnal values of the IMF are recorded during the summer most of the tine except between 21:00 LT and 22:00 LT, and between 04:00 LT and 06:00 LT where the lowest values are obtained in winter and in autumn respectively. During the solstices, the amplitudes of the diurnal values of the IMF in winter are greater than those of summer except between 21:00 LT and 22:00 LT. A strong fluctuation of the IMF is recorded during the four seasons during cycle 24. The equinoxes (spring and autumn) and the solstices (winter and summer) are asymmetrical during cycle 24 *i.e.* the values of IMF in autumn are generally lower than those of spring (**Figure 1(b)**) and the values of the IMF in winter are higher than those in summer (**Figure 1(b)**).

As an overview, we can say that the highest seasonal diurnal values of the interplanetary magnetic field are observed in autumn during the solar cycle 23 and in spring during solar cycle 24. The amplitudes of the interplanetary magnetic field during the solar cycle 24 are smaller than those of the solar cycle 23. The geomagnetic activity is strong at the spring and autumn equinoxes with different orientations of the IMF as reported in [17] [18] where ejections play important role in turbulence observe in solar wind propagation. The strong fluctuation of the interplanetary magnetic field during solar cycle 24 compared to solar cycle 23, may be explained by the large number of CMEs observed during solar cycle 24. As to the weak in the interplanetary magnetic field, it may be explained by the non-geoeffectiveness of the coronal mass ejections of solar cycle 24 and the drop of the polar fields after the deep minimum which followed solar cycle 23 [19] [20]).

Figure 2(a), presents the seasonal diurnal variation of proton density during solar cycle 23. In this figure, the highest diurnal values of proton density during solar cycle 23 are observed during the winter and the lowest are observed during the fall between 03:00 LT and 07:00 LT. Fluctuation of the proton density is fairly moderate during the four seasons during cycle 23. The solstices (winter and summer) are asymmetrical during cycle 23; the values of the proton density in winter are higher than those in summer (**Figure 2(a)**). However, during the equinoxes, there is a very remarkable asymmetry between 02:00 LT and 06:00 LT
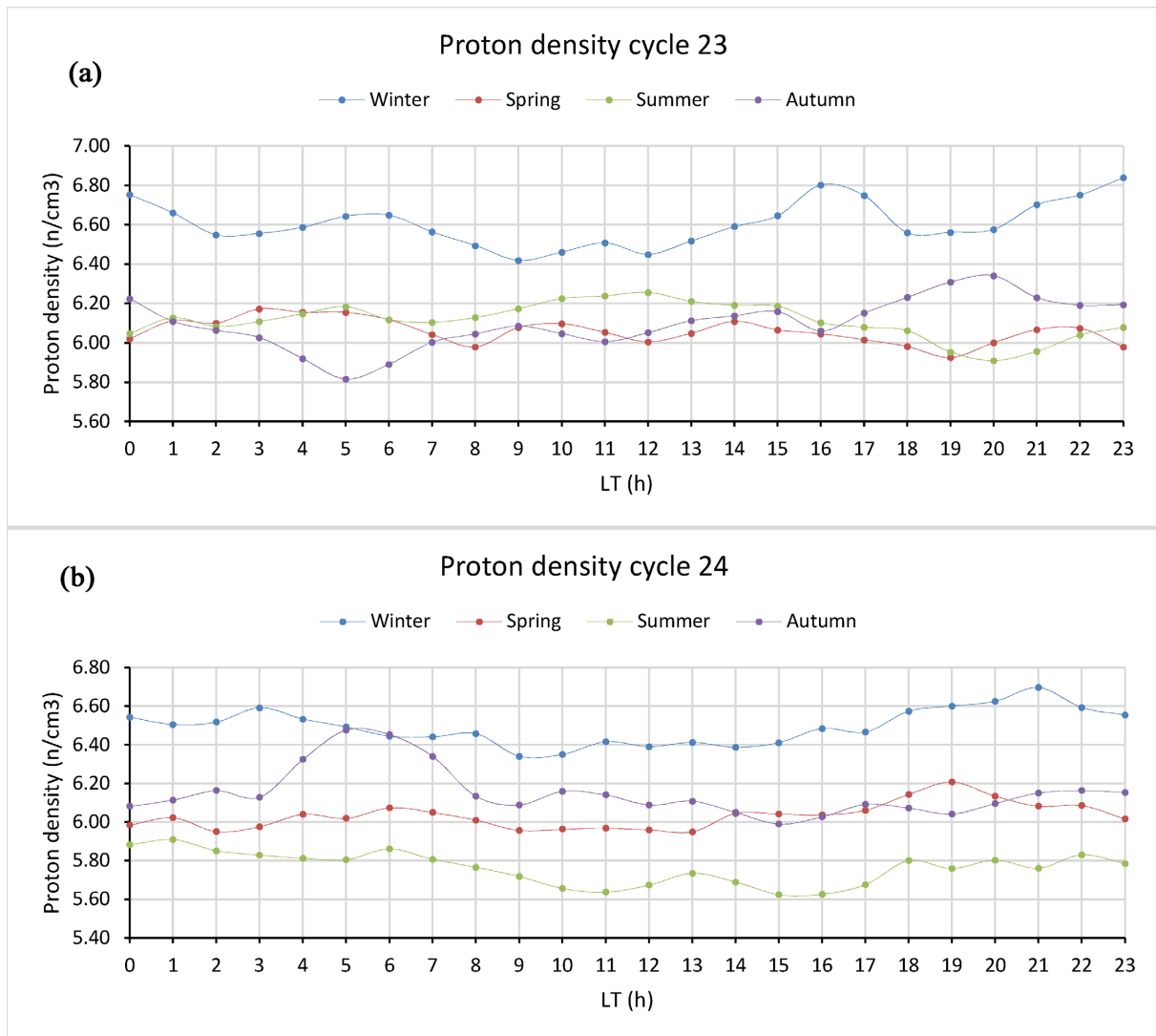
Figure 2. Diurnal seasonal variation of proton density during solar cycle 23 (a) and solar cycle 24 (b).

where the values of the proton density in spring are much important than those in autumn and reciprocally between 16:00 LT and 23:00 LT. During the other period of the day, a fairly low asymmetry of the seasonal diurnal values of the proton density is observed.

Figure 2(b) presents the diurnal seasonal variation of the proton density during the solar cycle 24. In this figure, the most important diurnal seasonal values of the proton density during the solar cycle 24 are observed during the winter. Low seasonal diurnal values are observed during summer. Moderate fluctuation of the proton density is observed during the four seasons during cycle 24, with exception for autumn where a strong daily fluctuation is observed between 03:00 LT and 08:00 LT. The solstices (winter and summer) are asymmetrical during cycle 24: the values of the proton density in winter are higher than those in summer (**Figure 2(b)**). During the equinoxes, there is a remarkable asymmetry between 00:00 LT and 13:00 LT; where the values of the proton density in au-

tumn are remarkably higher than those in spring (**Figure 2(b)**). We can then deduce that the highest seasonal diurnal values of proton density are observed in winter for both solar cycles. The lowest values are observed in autumn during the solar cycle 23 and in summer during the solar cycle 24.

Figure 3(a) presents the seasonal diurnal variation of the solar wind speed during solar cycle 23. This figure shows that the highest diurnal values of the solar wind speed are observed during spring while the lowest values are recorded during the summer. There is a slight fluctuation in solar wind speed during the four seasons for the solar cycle 23. The equinoxes (spring and autumn) and the solstices (winter and summer) are asymmetrical during cycle 23: the values of solar wind speed in spring are higher than those of autumn (**Figure 3(a)**) and the values of solar wind speed in winter are higher than those in summer (**Figure 3(a)**).

Figure 3(b) presents the seasonal diurnal variation of the solar wind speed
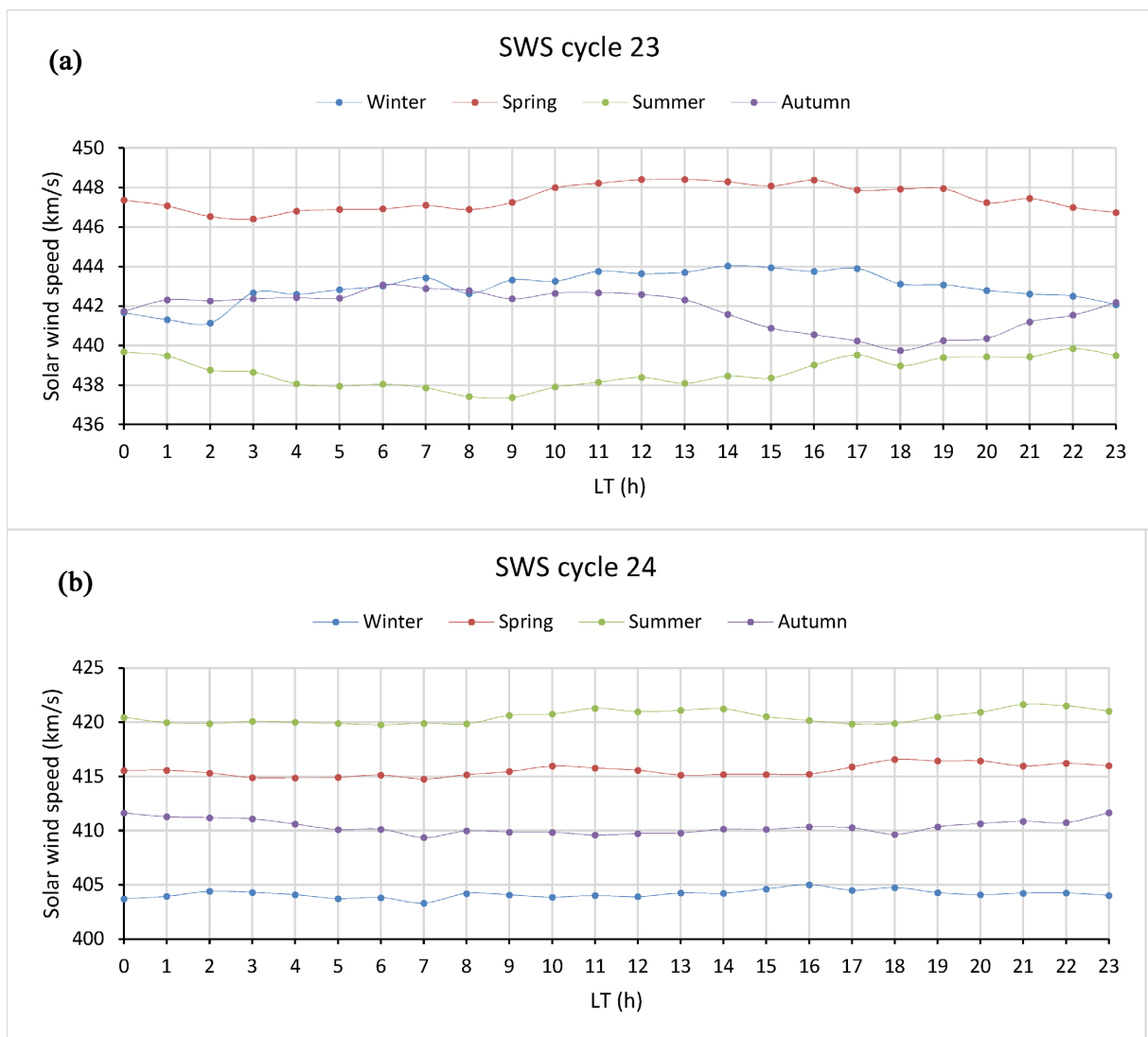
Figure 3. Diurnal seasonal variation of solar wind speed during solar cycle 23 (a) and solar cycle 24 (b).

during solar cycle 24. In this figure, the solar wind speed varies with season but present very little variation at the scale of hour during the four seasons. The largest diurnal amplitudes are observed during summer and the lowest during winter. Almost no fluctuation in the solar wind speed is recorded during the four seasons for the solar cycle 24. The equinoxes (spring and autumn) and solstices (winter and summer) are asymmetrical during cycle 24: the values of solar wind speed in spring are higher than those of autumn (Figure 3(b)) and the values of solar wind speed in summer are higher than those in winter (Figure 3(b)).

The lowest velocities are observed in summer during solar cycle 23 and winter during solar cycle 24. Compared to equinox's months, we can assume that the lowest velocities are observed most of the time during the solstices, with an exceptionally observation for solar cycle 24 where he highest and lowest diurnal values are recorded during the summer and winter respectively as reported by [16] who showed that low seasonal averages (<400 km/s) of the solar wind speed occur more often during the solstices than during the equinoxes. Moreover, the amplitudes of the solar wind speed during the four seasons during the solar cycle 24, are smaller compared to those of the solar cycle 23. This may be explained by the absence of persistent coronal holes during the solar cycle 24 responsible for high-speed flows [16] [21] [22] [23] [24], no equatorial and low latitude coronal holes have been observed during the deep solar minimum that followed the solar cycle 23 explaining why the slowest solar wind conditions of space age has been recorded during this solar cycle phase. Figure 4(a) shows the seasonal diurnal variation of the dynamic solar wind pressure during solar cycle 23. The solar wind dynamic pressure varies with the season and the time of day. The highest seasonal diurnal amplitudes of solar wind dynamic pressure are observed in winter with a peak at 06:00 LT and at 21:00 LT. On the other side, the lowest seasonal diurnal values are recorded during the summer. Additional observation shows that the diurnal amplitudes in winter are greater than in summer. As for the equinoxes, the seasonal diurnal amplitudes are greater during spring between 02:00 LT h and 06:00 LT than during autumn and vice-versa between 06:00 LT and 09:00 LT and between 17:00 LT and 23:00 LT in autumn than in spring. During the winter, we observe a decrease in the dynamic pressure of the solar wind from 00:00 LT to 02:00 LT then an increase from 03:00 LT before reaching a peak at 06:00 LT, then a decrease from 07:00 LT to 10:00 LT followed by an almost stable evolution between 10:00 LT and 12:00 LT, before starting to grow again from 12:00 LT, with a maximum obtained between 16:00 LT and 17:00 LT; from 20:00 LT there is a continuous growth until 23:00 LT. As for the summer, we observe an almost stable fluctuation of the daily values of the dynamic pressure of the solar wind from 00:00 LT to 09:00 LT, followed by a strong fluctuation from 10:00 LT with a maximum obtained around 12:00 LT; then a decrease until 21:00 LT followed by an increase from 21:00 LT to 23:00 LT. During spring and autumn, the daily dynamic pressure values of the solar wind vary inversely between 02:00 LT and 10:00 LT and between 17:00 LT and
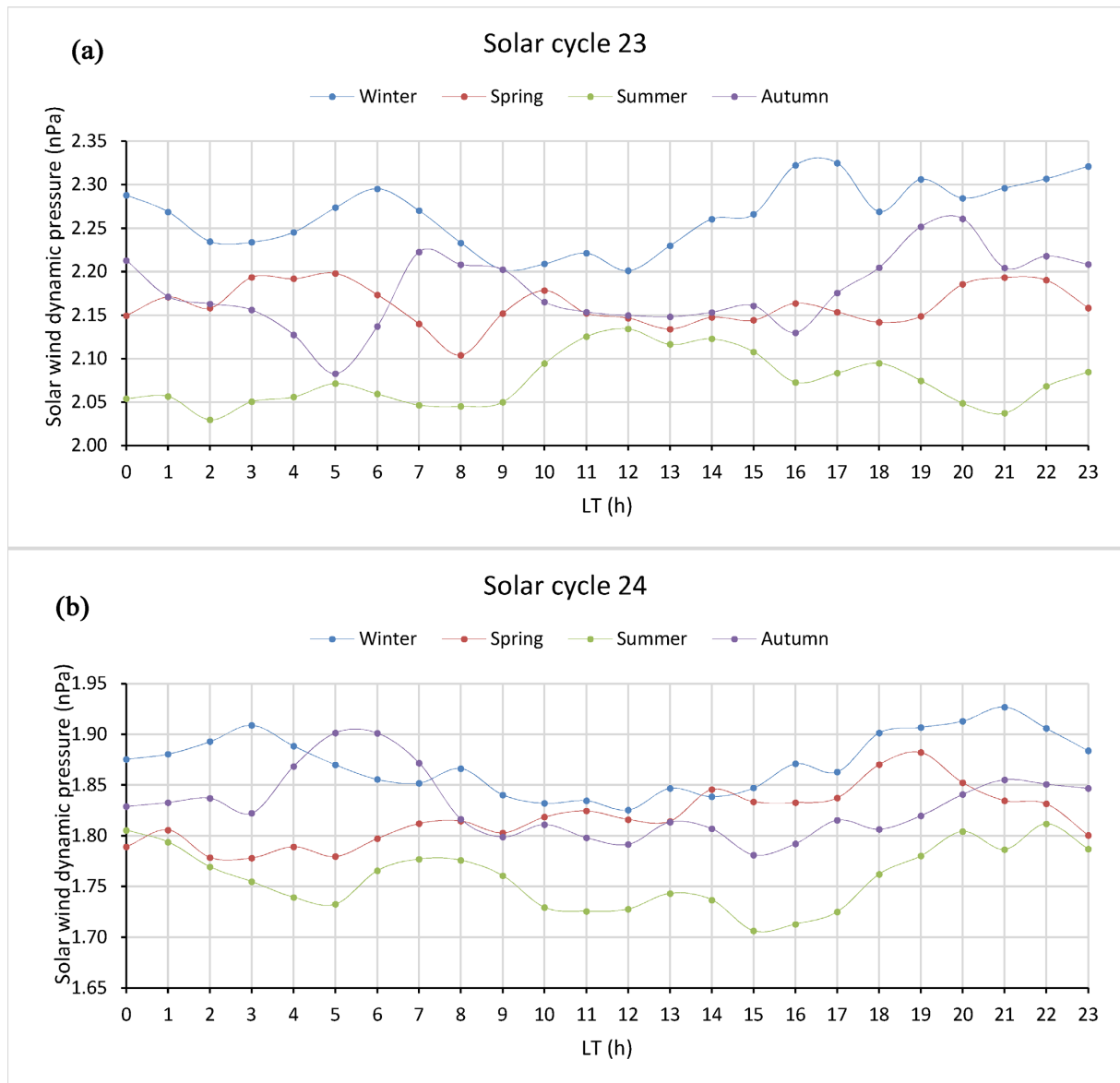
Figure 4. Diurnal seasonal variation of dynamic solar wind pressure during solar cycle 23 (a) and solar cycle 24 (b).

21:00 LT the spring maxima coincide with the autumn minima. A strong fluctuation in the dynamic pressure of the solar wind is recorded during the four seasons during cycle 23. The equinoxes (spring and autumn) and the solstices (winter and summer) are asymmetrical during cycle 23.

Figure 4(b), presents the seasonal diurnal variation of the dynamic solar wind pressure during the solar cycle 24. This figure shows that, the highest diurnal values of the dynamic solar wind pressure are obtained during the winter between 00:00 LT and 04:00 LT; 08:00 LT and 13:00 LT then between 15:00 LT and 023:00 LT and during the autumn between 05:00 LT and 07:00 LT. The lowest values are observed during the summer. During the solstices, the seasonal diurnal amplitudes are greater in winter than in summer. Moreover, during the equinoxes, the diurnal seasonal pressure amplitudes are greater between 00:00

LT and 08:00 LT in autumn than in spring with a peak between 05:00 LT and 06:00 LT and vice-versa in spring than in autumn between 14:00 LT and 19:00 LT. During winter, we observe an increase in the daily values of the dynamic pressure of the solar wind between 00:00 LT and 03:00 LT, then a decrease between 03:00 LT and 12:00 LT, before increasing again from 13:00 LT, with a peak at 21:00 LT before decreasing until 23:00 LT. During the summer, a decrease in the daily values of the dynamic pressure of the solar wind is observed between 00:00 LT and 05:00 LT, with An increase between 05:00 LT and 07:00 LT, before decreasing again from 08:00 LT to 15:00 LT, followed by an increase from 16:00 LT with a peak obtained at 22:00 LT, before decreasing again until 23:00 LT. During spring and autumn we observed a similar evolution of the daily averages of the solar wind dynamic pressure between 00:00 LT to 03:00 LT and between 08:00 LT to 23:00 LT, with the exception from 03:00 LT to 08:00 LT, where we observe a significant fluctuation in daily values during the autumn. A strong fluctuation in the dynamic pressure of the solar wind is recorded during the four seasons during cycle 24. The equinoxes (spring and autumn) and the solstices (winter and summer) are asymmetrical during this solar cycle.

From these observations it appears that: the highest seasonal diurnal values of dynamic solar wind pressure are observed at the winter solstice during both solar cycles; with greater amplitudes during solar cycle 23 than during solar cycle 24, during the four seasons. Also, the lowest dynamic solar wind pressures are observed during the summer solstice in both solar cycles 23 and 24.

To better understand the seasonal asymmetries, we calculated the relative differences or relative deviations of the months of equinoxes and solstices of the different parameters of the solar wind during the two solar cycles shown in Figures 5-8.

Figure 5 presents the variations in the difference of the IMF between the solstice months ($\Delta IMF_{-Solstice}$) and the equinox months ($\Delta IMF_{-Equinox}$) during the solar cycles 23 and 24. In Figure 5(a) and Figure 5(b), $\Delta IMF_{-Solstice}$ and $\Delta IMF_{-Equinox}$ are negative throughout the day with respective maximum values of −7.45% around 06:00 LT for the solstices and −6.03% around 21:00 LT for the equinoxes. The daily values in summer are lower than those in winter; similarly, the daily values in spring are smaller than those in autumn, during solar cycle 23. During solar cycle 24, $\Delta IMF_{-Solstice}$ (Figure 5(c)) is negative, except between 3h and 5 h and between 21:00 LT and 23:00 LT, where they are positive; $\Delta IMF_{-Equinox}$ (Figure 5(d)) are positive, except between 12 h and 16 h. This means that during the solstices, the daily values of the interplanetary magnetic field of summer are smaller than those of winter, except between 03:00 LT and 05:00 LT and between 21:00 LT and 23:00 LT; likewise during the equinoxes, the daily values of the equinox are smaller in autumn than in spring, except between 12:00 LT and 16:00 LT. All these results clearly show an asymmetry in the daily values of the interplanetary magnetic field at the equinoxes and solstices during solar cycles 23 and 24.

Figure 6 shows the variations in the deviation of the proton density of the
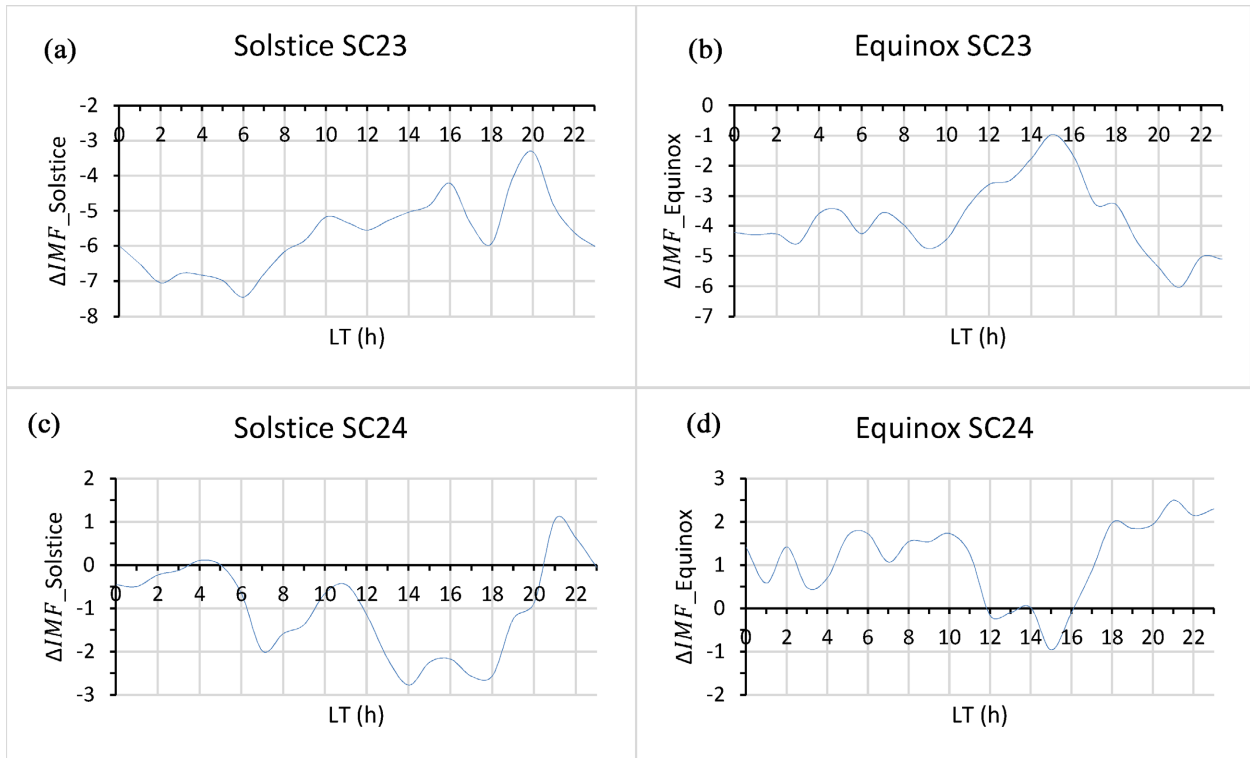
Figure 5. Variations of difference between the months of solstices ($\Delta IMF_{-Solstice}$) and the months of equinox ($\Delta IMF_{-Equinox}$) during solar cycle 23 (a) and (b) and solar cycle 24 (c) and (d).
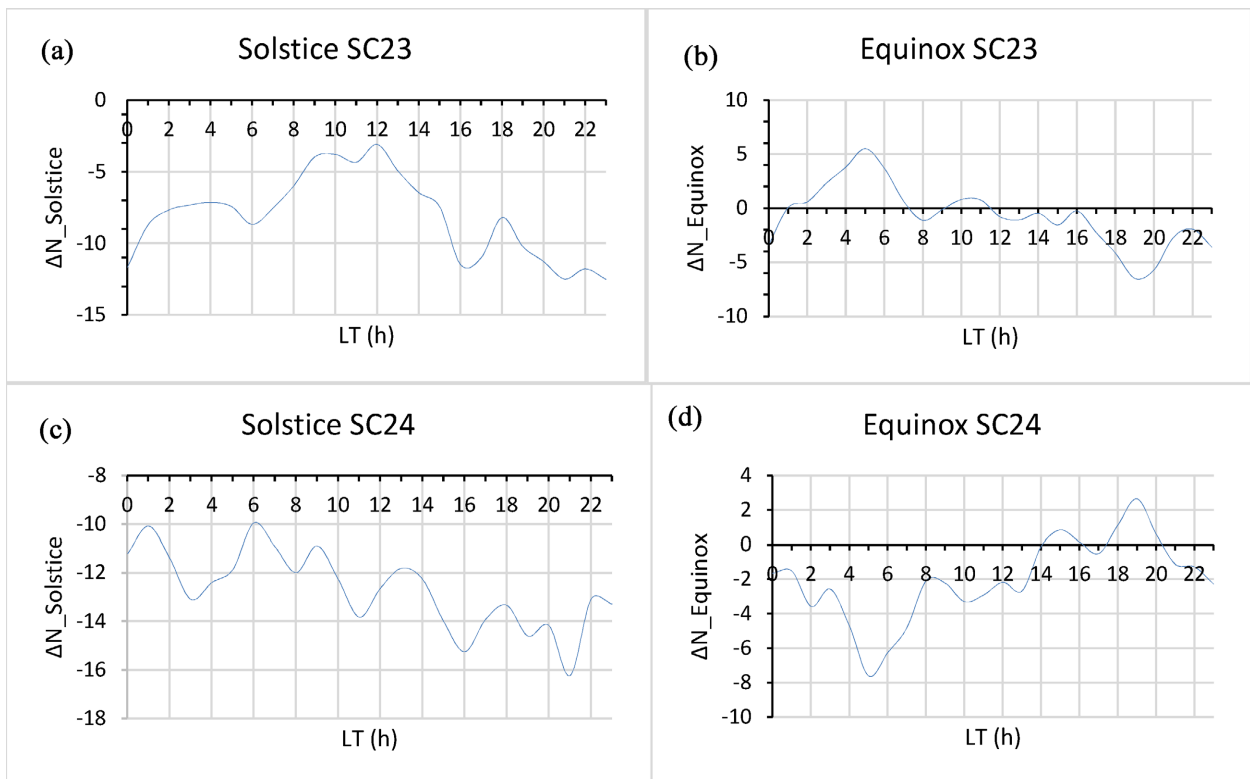
Figure 6. Variations in the difference between the months of solstices (ΔN_Solstice) and equinoxes (ΔN-Equinox) during solar cycle 23 (a) and (b) and solar cycle 24 (c) and (d).

months of solstices (**Figures 6(a)-(c)**) and equinoxes (**Figures 6(b)-(d)**) during solar cycles 23 and 24. The ΔN_Solstice (**Figures 6(a)-(c)**), are negative throughout the day; for ΔN-Equinox (**Figures 6(b)-(d)**), a negative variation is observed between 00:00 LT and 01:00 LT; at 08:00 LT and between 12:00 LT and 23:00 LT with an extreme of −6.48% around 19:00 LT and a positive variation between 01:00 LT and 06:00 LT with a maximum of 5.51% around 05:00 LT. During the solstices, the daily values of the proton density are smaller in summer than winter; during the equinoxes, the daily values of the proton density in spring are smaller between 00:00 LT and01:00 LT; at 08:00 LT and between 12:00 LT and 23:00 LT and larger between 01:00 LT and 06:00 LT than those of autumn. During solar cycle 24, the ΔN-solstices are negative throughout the day; which indicates that the values of the proton density of the summer are smaller than those of the winter. During the equinoxes the daily values of the density of proton in spring are smaller between 00:00 LT and 14:00 LT; around 17:00 LT and between 21:00 LT and 23:00 LT and larger between 14:00 LT and 16:00 LT and between 18:00 LT and 20:00 LT than those of the autumn.

Figure 7 shows the variations in the deviation of the solar wind speed of the months of solstices (**Figure 7(a)** and **Figure 7(c)**) and equinoxes (**Figure 7(b)** and **Figure 7(d)**) during the solar cycle 23 and 24. In these figures, we observe clearly that during the solstices (**Figure 7(a)** and **Figure 7(c)**), the daily values of
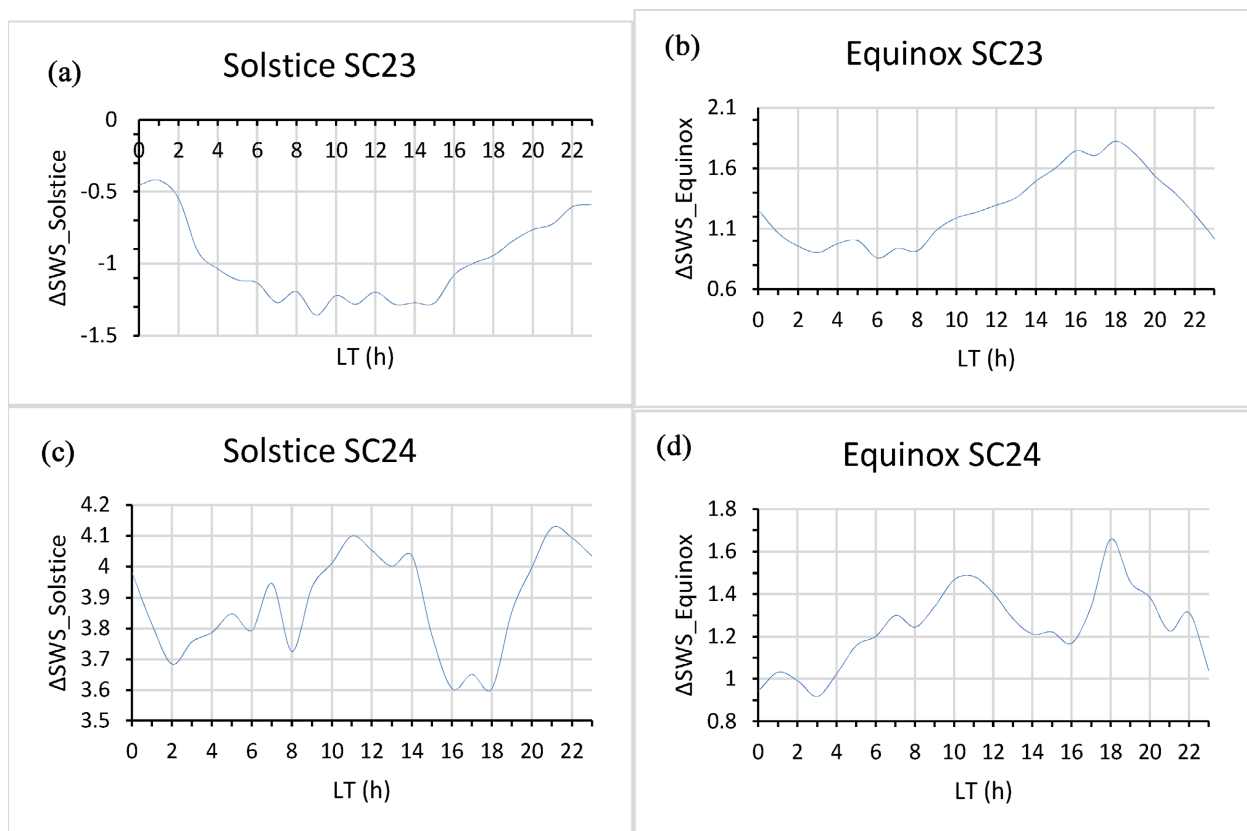
Figure 7. Variations in the difference between the months of solstices (ΔSWS_Solstice) and equinoxes (ΔSWS_Equinox) during solar cycle 23 (a) and (b) and during solar cycle 24 (c) and (d).

the summer solar wind speed are smaller during the solar cycle 23 and larger during solar cycle 24, than those of winter. During the equinoxes (**Figure 7(b)** and **Figure 7(d)**) in both cycles, the daily values of the solar wind speed during the spring are greater than those of the autumn, with a maximum of 1.82% and 1.65% respectively at cycles 23 and 24, around 18:00 LT.

Figure 8 presents the variations in the deviation of the dynamic pressure of the solar wind during the months of solstices (**Figure 8(a)** and **Figure 8(c)**) and equinoxes (**Figure 8(b)** and **Figure 8(d)**) during the solar cycle 23 and 24. During the solstices (**Figure 8(a)** and **Figure 8(c)**), the daily values of the dynamic solar wind pressure of summer are smaller than those of winter during solar cycles 23 and 24. During the equinoxes (**Figure 8(b)** and **Figure 8(d)**), the daily values of the dynamic pressure of the solar wind in the spring are smaller from 00:00 LT and 01:00 LT; from 07:00 LT and 09:00 LT; from 12:00 LT and 15:00 LT and 17:00 LT and 20:00 LT and greater from 02:00 LT and 06:00 LT; around 10:00 LT and 16:00 LT than those in the autumn. During the equinoxes in solar cycle 24, the daily values of dynamic solar wind pressure in spring are smaller between 00:00 LT and 08:00 LT and between 21:00 LT and 23:00 LT and larger between 08:00 LT and 20:00 LT than those in autumn.

3.2. Annual Seasonal Variations

Figure 9(a) and **Figure 9(b)**, present the seasonal variations at the equinoxes and at the solstices of the interplanetary magnetic field during solar cycles 23
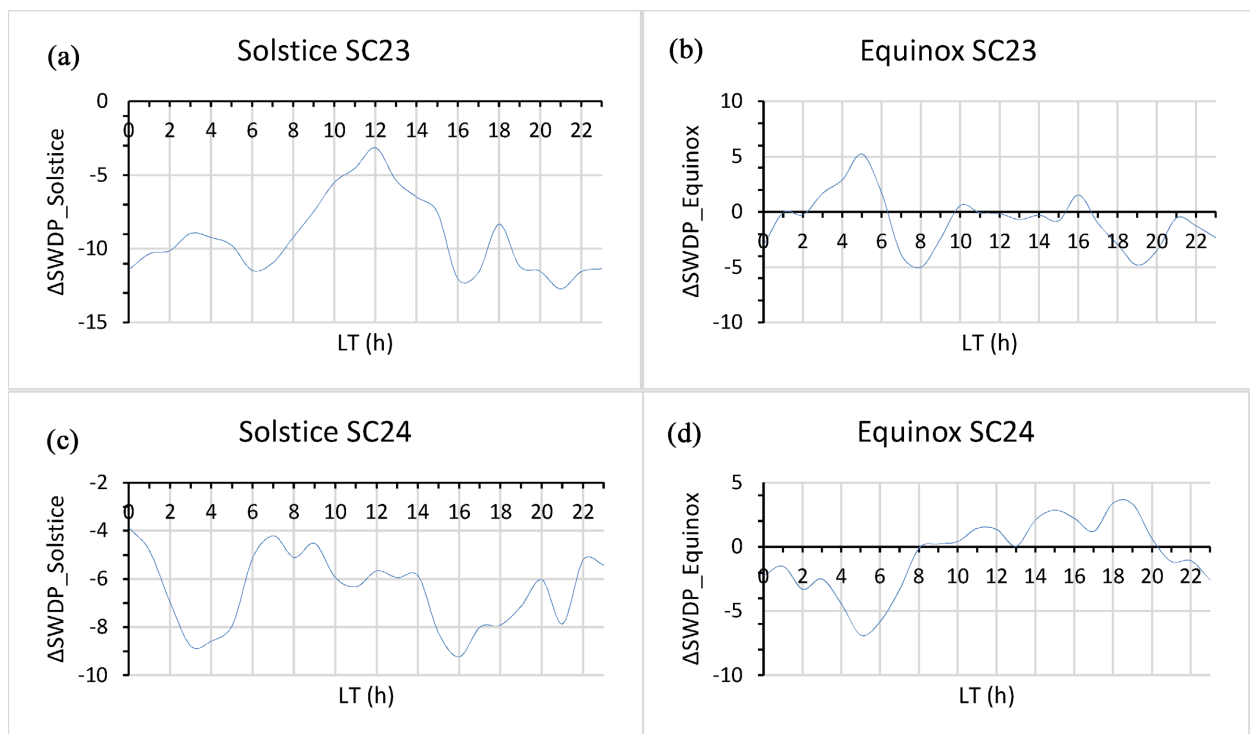
Figure 8. Variations in the difference between the months of solstices (ΔSWDP_Solstice) and equinoxes (ΔSWDP_Equinox) during solar cycle 23 (a) and (b) and during solar cycle 24 (c) and (d).

and 24 covering the period 1996 to 2019. During the solar cycle 23, we observe several peaks in the interplanetary magnetic field variation before and after the solar maximum at the summer solstices (**Figure 9(b)**), with several troughs. At the winter solstices, a double peak is observed: the first peak occurred in 1999 (7.28 nT) and the second peak in 2003 (7.86 nT). At the equinoxes (**Figure 9(a)**), a double peak structure is observed, with a shift of the first peak during spring and during summer, obtained respectively in 1998 (7.14 nT) in spring and in 2000 (7.42 nT) in autumn. The second peaks are obtained in 2002 with respective values of 7.77 nT during spring and 8.48 nT during autumn. We also notice a rapid reversal of the polarity of the magnetic field during the spring (1998).

During the solar cycle 24, a double-peak variation of the interplanetary magnetic field at the equinoxes and at the solstices (**Figure 9(a)** and **Figure 9(b)**) is observed. At the equinoxes (**Figure 9(a)**), we observe a shift in the maxima of the two peaks during spring and autumn; the first peak is obtained in 2012 (5.75 nT) and the second in 2015 (6.74 nT), on the other side, the first peak of the autumn is obtained in 2011 (5.64 nT) and the second peak in 2014 (6.97 nT). At the solstices (**Figure 9(b)**), the first peak of the interplanetary magnetic field in
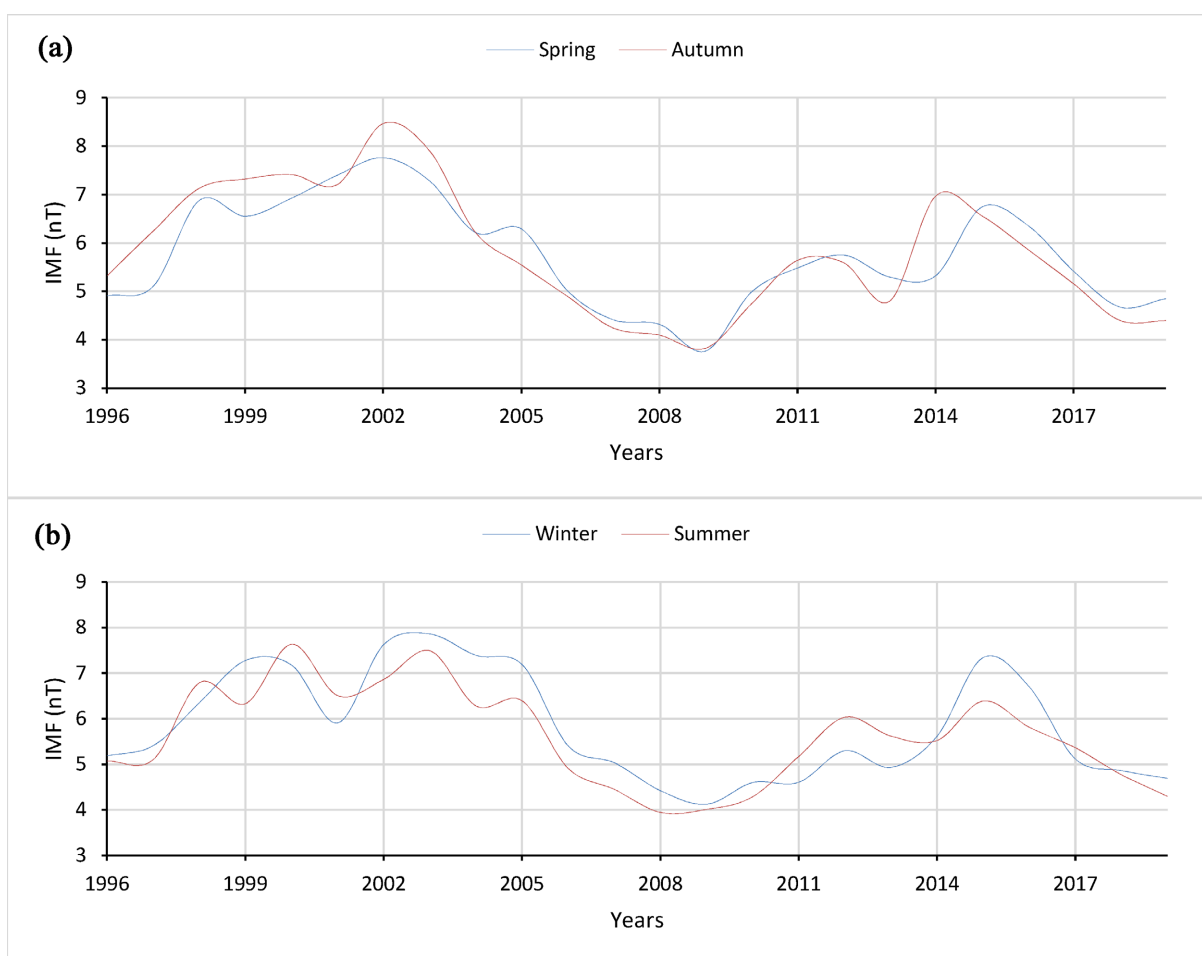
Figure 9. Seasonal variation at the equinoxes (a) and solstices (b) of the interplanetary magnetic field during solar cycles 23 and 24.

winter and in summer is obtained at exactly the same period (2012) with different amplitudes; respective values of 5.30 nT in winter and 6.04 nT in summer. The second peak is observed in 2015, with respective amplitudes of 7.35 nT in winter and 6.39 nT in summer. There is also a shift in the troughs between the peaks during the two seasons. These troughs represent the period of reversal of the polarity of the magnetic field. During the equinoxes, there is a one-year shift during the change of polarity in spring and autumn; similarly during the solstices, there is also a shift in the troughs during summer and winter. In addition, there is a rapid polarity change during the winter and a prolonged polarity change during the summer.

The highest values of the interplanetary magnetic field are observed at the equinoxes (in autumn) during solar cycle 23 and solstices (winter) during solar cycle 24. During the deep minimum that followed the solar cycle 23, the interplanetary magnetic field presents a similar evolution at the equinox months. The equinoxes (spring and autumn) and solstices (summer and winter) are asymmetrical during the two solar cycles; the values of the interplanetary magnetic field at the solstices during solar cycle 23 are higher than those of solar cycle 24 and the values of the interplanetary magnetic field at the equinoxes during solar cycle 23 are higher than those of solar cycle 24. Additionally, we see that polar field intensities remained in the ~6 - 9 nT range during the 1976, 1986, and 1996 sunspot minima, but fell to only ~4 - 5 nT during the current minimum [25] [26] [27] [28] and remained weak during the current solar maximum (2014). It should be noted that the variation in magnetic activity during the course of the 11-year cycle influences not only the sunspot number and the magnetic flux but also the radiation emitted by the Sun and that we receive on Earth called total irradiance or "solar constant" [29]). This indeed varies in phase with the solar cycle by approximately 0.1%: the higher the number of spots, the higher the flux that we receive from the Sun, due to the massive presence of faculae which are more brilliant [30].

Figure 10(a) and Figure 10(b) present the seasonal variations at the equinoxes and at the solstices of the proton density during solar cycles 23 and 24. A strong fluctuation of the proton density at the equinoxes and at the solstices is observed during of the two solar cycles. During the equinoxes, the maximum values of the proton density are recorded in spring respectively in 1997 (9.17 n/cm^3) during solar cycle 23 and in 2015 (7.55 n/cm^3) during solar cycle 24. During the solstices, the maximum values of the proton density are recorded during the winter respectively in 1998 (9.31 n/cm^3) during solar cycle 23 and in 2018 (7.73 n/cm^3) during solar cycle 24. In generally we observe a random variation of the density of proton at the solstices (summer and winter) and at the equinoxes (spring and autumn) during the two solar cycles.

Figure 11(a) and Figure 11(b) present the seasonal variations at the equinoxes and solstices of the solar wind speed during solar cycles 23 and 24. During solar cycle 23, the maximum values of the speed at the equinoxes are enough similar, but during the solstices the maximum values are different during summer
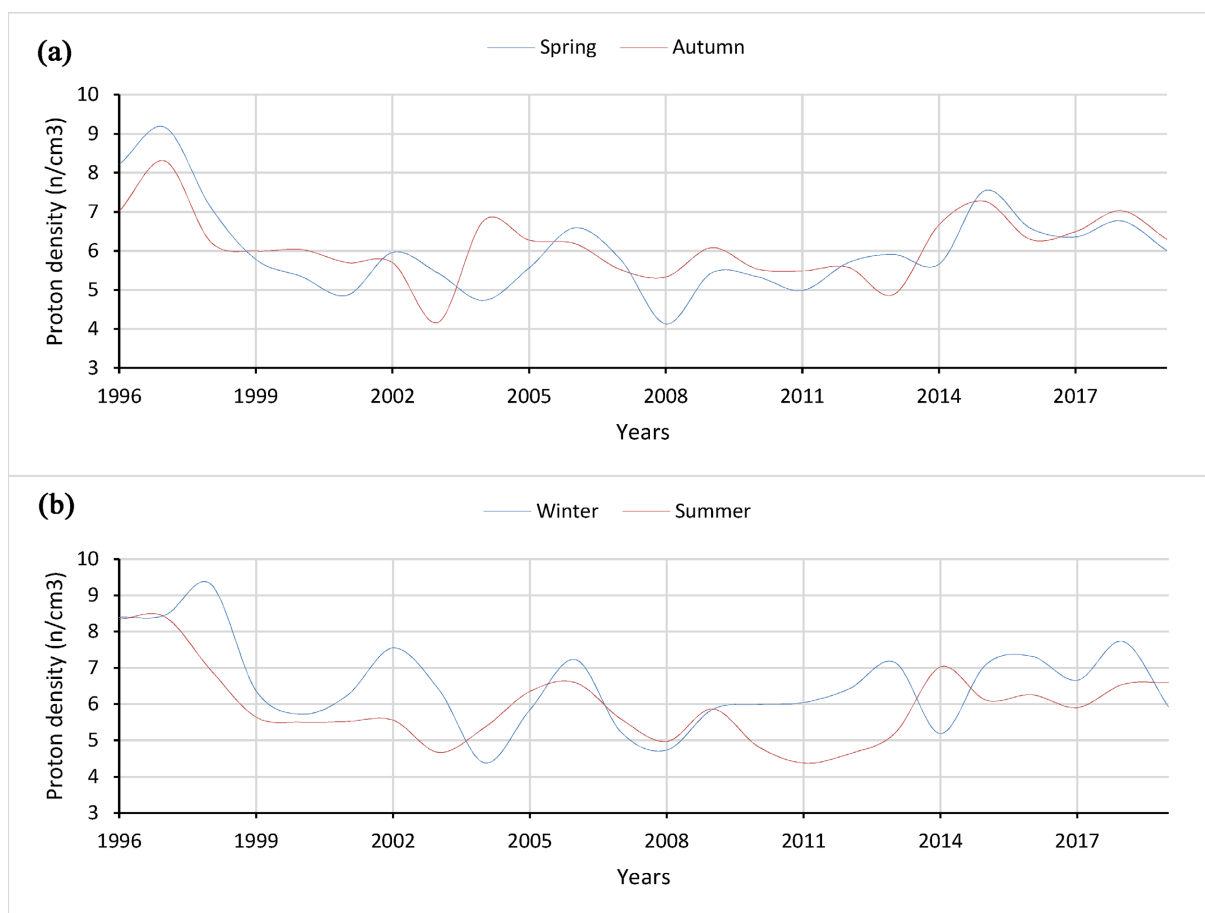
Figure 10. Seasonal variation at the equinoxes (a) and solstices (b) of the proton density during solar cycles 23 and 24.

and winter. The maximum values at the equinoxes are respectively 548.41 Km/s obtained in spring 2003 and 541.42 km/s obtained in autumn 2003. During the solstices, the maximum values are respectively 580.67 Km/s obtained in summer 2003 and 515.15 km/s obtained in winter 2015. During solar cycle 24, the solar wind speed reaches roughly equal maximum values during the solstices and equinoxes. The maximum value at the solstices is obtained in winter 2017 (475.75 km/s) and that at the equinoxes is obtained in autumn 2016 (463.49 km/s). During low cycles, solar wind speeds reached roughly similar maximum values of about 460-470 km/s in both seasons [16].

The equinoxes (spring and autumn) and solstices (summer and winter) are asymmetrical during the two solar cycles; the values of the solar wind speed at the solstices during solar cycle 23 are higher than those of solar cycle 24 and the values of the solar wind speed at the equinoxes during solar cycle 23 are higher than those of solar cycle 24. The continued presence of so many low-latitude holes so late in cycle 23, with recurring high-velocity flows persisting in the ecliptic until early 2009, is therefore another consequence of weak polar fields [25]. Based on an analysis of Ulysses plasma measurements taken between 2006 and 2008, [2] found that the wind from the polar hole was ~17% less dense and ~14% colder than during the previous solar minimum; the wind speed was only
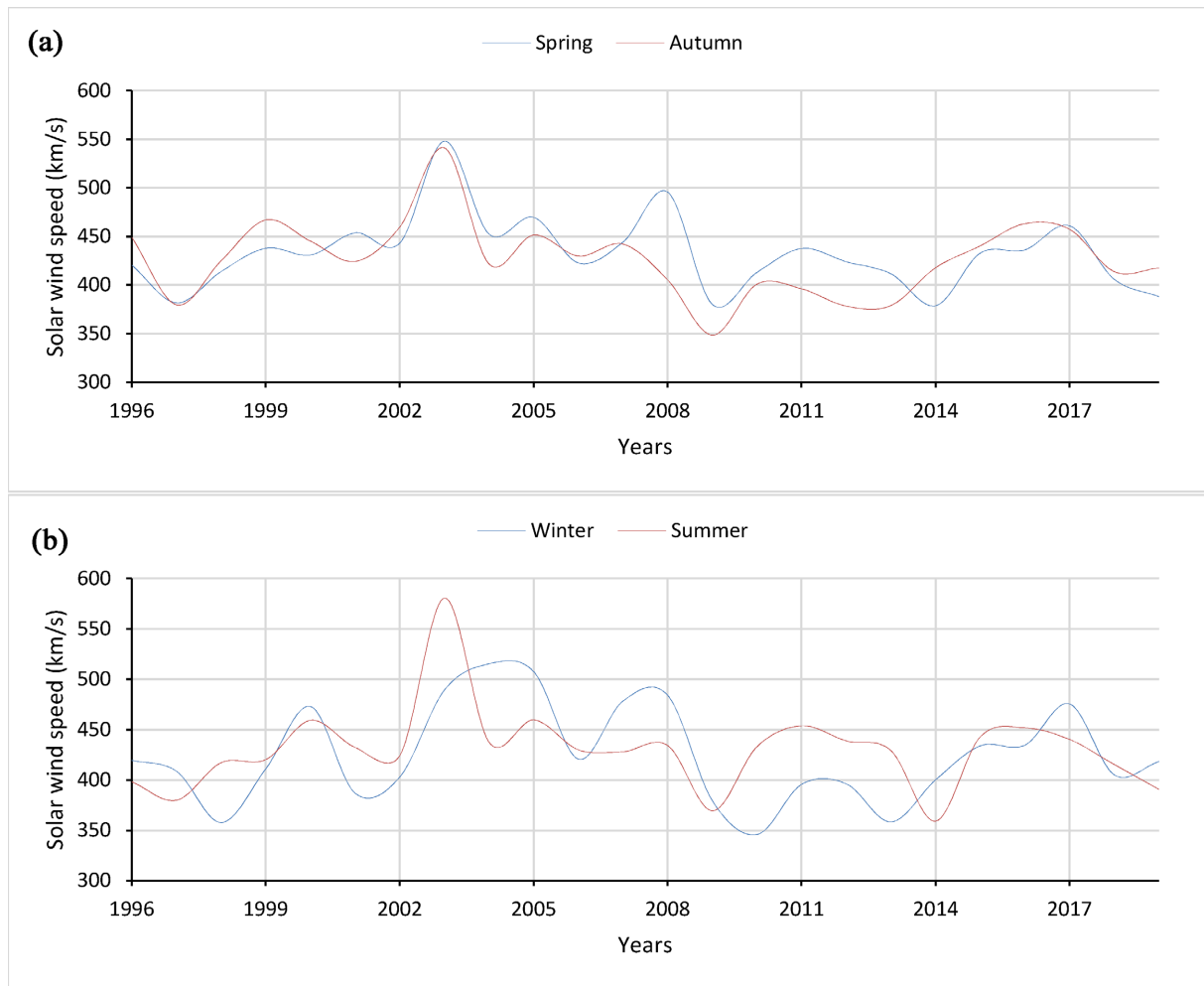
Figure 11. Seasonal variation at the equinoxes (a) and solstices (b) of the solar wind speed during solar cycles 23 and 24.

about 3% lower, but the proton flux density was about 20% lower.

Figure 12(a) and **Figure 12(b)** present the seasonal variations at the equinoxes and solstices of the solar wind dynamic pressure during solar cycles 23 and 24. During the equinoxes (**Figure 12(a)**), the highest solar wind dynamic pressures values are observed during spring respectively in 2003 (3.06 nPa) during solar cycle 23 and in 2015 (2.56 nPa) during solar cycle 24. During the solstices (**Figure 12(b)**), a strong fluctuation of solar wind dynamic pressure during solar cycle 23 compared to solar cycle 24; the maximum values are observed respectively in 2005 (2.84 nPa) during solar cycle 23 and 2015 (2.52 nPa) during solar cycle 24.

The equinoxes (spring and autumn) and solstices (summer and winter) are asymmetrical during the two solar cycles; the values of the solar wind dynamic pressure at the solstices during the solar cycle 23 are higher than those of the solar cycle 24 and the values of the solar wind dynamic pressure at the equinoxes during the solar cycle 23 are higher than those of the solar cycle 24.

From **Figures 9-12**, it appears that the deep minimum that followed solar cycle 23 can be seen in both the solar wind parameters at the solstices and the
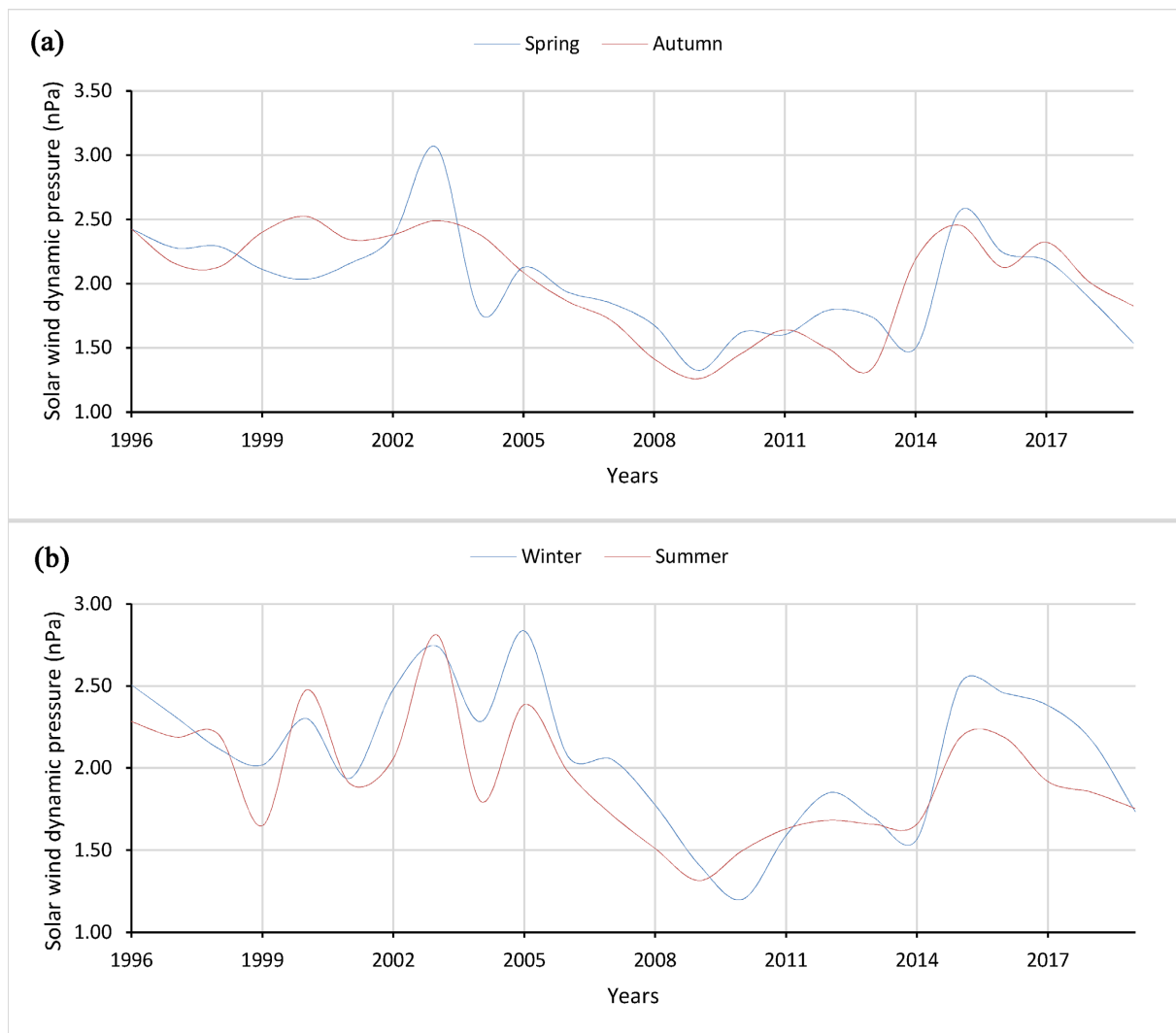
Figure 12. Seasonal variation at the equinoxes and solstices of the dynamic pressure of the solar wind during solar cycles 23 and 24.

equinoxes. During this deep minimum there is a general drop in solar wind's parameters. This constant change in solar wind may have a great effects on Earth as reviewed by [31] when investigating variation in solar activity and its climatic impact on Earth.

4. Conclusions

We analyzed diurnal seasonal variations as well as annual seasonal variations of solar wind parameters such as interplanetary magnetic field, proton density, solar wind speed and dynamic solar wind pressure during solar cycles 23 and 24. Our study shows that:

- Strong geomagnetic disturbances are observed at the equinoxes during both solar cycles 23 and 24.
- The highest proton densities are observed at solstices during both solar cycles.

- The greatest solar wind speeds are observed at the equinoxes during solar cycle 23 and at the solstices during solar cycle 24.
- The greatest dynamic solar wind pressures are observed at the solstices during both solar cycles.
- A very remarkable asymmetrical evolution of the seasonal diurnal values of the solar wind parameters is observed during the two cycles, except for the proton density where during the equinoxes, it varies according to the hours of the day.
- Seasonal diurnal values of solar wind parameters are significant at solar cycle 23 compared to solar cycle 24; with a strong fluctuation of the interplanetary magnetic field and quasi-stable and low seasonal diurnal velocities during cycle 24. His observations during solar cycle 24 are explained by the weakening of the polar fields during solar cycle 23 and after the deep minimum that followed leading to an absence of persistent polar coronal hole.

Acknowledgements

Conflicts of Interest

The authors declare no conflicts of interest regarding the publication of this paper.

References

[1] Wang, Y.-M., Sheeley Jr., N.R., and Nash, A.G. (1991) A New Solar Cycle Model Including Meridional Circulation. *The Astrophysical Journal*, **383**, 431-442. https://doi.org/10.1086/170800

[2] McComas, D.J., Ebert, R.W., Elliott, H.A., Goldstein, B.E., Gosling, J.T., Schwadron, N.A. and Skoug, R.M. (2008) Weaker Solar Wind from the Polar Coronal Holes and the Whole Sun. *Geophysical Research Letters*, **35**, L18103. https://doi.org/10.1029/2008GL034896

[3] Pinto, R.F., Brun, A.S., Jouve, L. and Grappin, R. (2011) Coupling the Solar Dynamo and the Corona: Wind Properties, Mass, and Momentum Losses during an Activity Cycle. *The Astrophysical Journal*, **737**, Article 72. https://doi.org/10.1088/0004-637X/737/2/72

[4] Parker, E.N. (1958) Dynamics of the Interplanetary Gas and Magnetic Fields. *The Astrophysical Journal*, **128**, 664. https://doi.org/10.1086/146579

[5] Legrand, J.P. and Simon, P.A. (1989) Solar Cycle and Geomagnetic Activity: A Review for Geophysicists. Part 1. The Contributions to Geomagnetic Activity of Shock Waves and of the Solar Wind. *Annales Geophysicae*, **7**, 565-593.

[6] Legrand, J.P., Le Goff, M. and Amory-Mazaudier, C. (1990) On the Climatic Changes and the Sunspot Activity during the XVIIth Century. *Annales Geophysi-*

cae, **8**, 637-644.

[7] Zerbo, J.L., Amory-Mazaudier, C., Frédéric, O. and Richardson, J.D. (2012) Solar Wind and Geomagnetism: Toward a Standard Classification of Geomagnetic Activity from 1868 to 2009. *Annales Geophysicae*, **30**, 421-426. https://doi.org/10.5194/angeo-30-421-2012

[8] D'Amicis, R., Telloni, D. and Bruno, R. (2020) The Effect of Solar-Wind Turbulence on Magnetospheric Activity. *Frontiers in Physics*, **8**, Article 604857. https://doi.org/10.3389/fphy.2020.604857

[9] Richardson, I.G., Webb, D.F., Zhang, J., Berdichevsky, D.B., Biesecker, D.A., Kasper, J.C., Kataoka, R., Steinberg, J.T., Thompson, B.J., Wu, C.-C. and Zhukov, A.N. (2006) Major Geomagnetic Storms (Dst ≤ −100 nT) Generated by Corotating Interaction Regions. *Journal of Geophysical Research*: *Space Physics*, **111**, A07S09. https://doi.org/10.1029/2005JA011476

[10] Zhang, J., Richardson, I.G., Webb, D.F., Gopalswamy, N., Huttunen, E., Kasper, J.C., Nitta, N.V., Poomvises, W., Thompson, B.J., Wu, C.-C., Yashiro, S. and Zhukov, A.N. (2007) Solar and Interplanetary Sources of Major Geomagnetic Storms (Dst ≤ −100 nT) during 1996-2005. *Journal of Geophysical Research*: *Space Physics*, **112**, A10102. https://doi.org/10.1029/2007JA012321

[11] Gosling, J.T., Asbridge, J.R., Bame, S.J. and Feldman, W.C. (1976) Solar Wind Speed Variations: 1962-1974. *Journal of Geophysical Research*, **81**, 5061-5070. https://doi.org/10.1029/JA081i028p05061

[12] Hakamada, K. and Akasofu, S.I. (1981) A Cause of Solar Wind Speed Variations Observed at 1 A.U. *Journal of Geophysical Research*: *Space Physics*, **86**, 1290-1298. https://doi.org/10.1029/JA086iA03p01290

[13] Harvey, J.W. and Sheeley, N.R. (1979) Coronal Holes and Solar Magnetic Fields. *Space Science Reviews*, **23**, 139-158. https://doi.org/10.1007/BF00173808

[14] Mursula, K. and Zieger, B. (1996) The 13.5-day Periodicity in the Sun, Solar Wind, and Geomagnetic Activity: The last Three Solar Cycles. *Journal of Geophysical Research*: *Space Physics*, **101**, 27077-27090. https://doi.org/10.1029/96JA02470

[15] Mursula, K. and Zieger, B. (2001) Long-Term North-South Asymmetry in Solar Wind Speed Inferred from Geomagnetic Activity: A New Type of Century-Scale Solar Oscillation? *Geophysical Research Letters*, **28**, 95-98. https://doi.org/10.1029/2000GL011880

[16] Mursula, K., Holappa, L. and Lukianova, R. (2017) Seasonal Solar Wind Speeds for the Last 100 Years: Unique Coronal Hole Structures during the Peak and Demise of the Grand Modern Maximum. *Geophysical Research Letters*, **44**, 30-36. https://doi.org/10.1002/2016GL071573

[17] Zhao, H. and Zong, Q.G. (2012) Seasonal and Diurnal Variation of Geomagnetic Activity: Russell-McPherron Effect during Different IMF Polarity and/or Extreme Solar Wind Conditions. *Journal of Geophysical Research*: *Space Physics*, **117**, A11222. https://doi.org/10.1029/2012JA017845

[18] Barkhatov, N.A., Revunova, E.A. and Vinogradov, A.B. (2014) Effect of Orientation of the Solar Wind Magnetic Clouds on the Seasonal Variation of Geomagnetic Activity. *Cosmic Research*, **52**, 269-277. https://doi.org/10.1134/S0010952514040017

[19] Schrijver, C.J. and Liu, Y. (2008) The Global Solar Magnetic Field Through a Full Sunspot Cycle: Observations and Model Results. *Solar Physics*, **252**, 19-31. https://doi.org/10.1007/s11207-008-9240-6

[20] Hathaway, D.H. and Upton, L. (2014) The Solar Meridional Circulation and Suns-

pot Cycle Variability. *Journal of Geophysical Research*: *Space Physics*, **119**, 3316-3324. https://doi.org/10.1002/2013JA019432

[21] Vennerstrom, S., Lefevre, L., Dumbović, M., Crosby, N., Malandraki, O., Patsou, I., Clette, F., Veronig, A., Vršnak, B., Leer, K. and Moretto, T. (2016) Extreme Geomagnetic Storms-1868-2010. *Solar Physics*, **291**, 1447-1481. https://doi.org/10.1007/s11207-016-0897-y

[22] Gosling, J.T., Bame, S.J., McComas, D.J. and Phillips, J.L. (1990) Coronal Mass Ejections and Large Geomagnetic Storms. *Geophysical Research Letters*, **17**, 901-904. https://doi.org/10.1029/GL017i007p00901

[23] Gonzalez, W.D., Echer, E., Clua-Gonzalez, A.L. and Tsurutani, B.T. (2007) Interplanetary Origin of Intense Geomagnetic Storms (Dst < −100 nT) during Solar Cycle 23. *Geophysical Research Letters*, **34**, L06101. https://doi.org/10.1029/2006GL028879

[24] Tsurutani, B.T., Echer, E., Guarnieri, F.L. and Gonzalez, W.D. (2011) The Properties of Two Solar Wind High Speed Streams and Related Geomagnetic Activity during the Declining Phase of Solar Cycle 23. *Journal of Atmospheric and Solar-Terrestrial Physics*, **73**, 164-177. https://doi.org/10.1016/j.jastp.2010.04.003

[25] Wang, Y.M., Robbrecht, E. and Sheeley, N.R. (2009) On the Weakening of the Polar Magnetic Fields during Solar Cycle 23. *The Astrophysical Journal*, **707**, 1372-1386. https://doi.org/10.1088/0004-637X/707/2/1372

[26] Owens, M.J., Arge, C.N., Crooker, N.U., Schwadron, N.A. and Horbury, T.S. (2008) Estimating Total Heliospheric Magnetic Flux from Single-Point *in Situ* Measurements. *Journal of Geophysical Research*: *Space Physics*, 113, A12103. https://doi.org/10.1029/2008JA013677

[27] Owens, M.J., Crooker, N.U., Schwadron, N.A., Horbury, T.S., Yashiro, S., Xie, H., Cyr, O.C.S. and Gopalswamy, N. (2008) Conservation of Open Solar Magnetic Flux and the Floor in the Heliospheric Magnetic Field. *Geophysical Research Letters*, **35**, L20108. https://doi.org/10.1029/2008GL035813

[28] Zerbo, J.L. and Richardson, J.D. (2015) The Solar Wind during Current and Past Solar Minima and Maxima. *Journal of Geophysical Research*: *Space Physics*, **120**, 10250-10256. https://doi.org/10.1002/2015JA021407

[29] Bard, E. and Frank, M. (2006) Climate Change and Solar Variability: What's New under the Sun? *Earth and Planetary Science Letters*, **248**, 1-14. https://doi.org/10.1016/j.epsl.2006.06.016

[30] Lean, J., Rottman, G., Harder, J. and Kopp, G. (2005) SORCE Contributions to New Understanding of Global Change and Solar Variability. In: Rottman, G., Woods, T. and George, V., Eds., *The Solar Radiation and Climate Experiment* (*SORCE*): *Mission Description and Early Results*, Springer, New York, 27-53. https://doi.org/10.1007/0-387-37625-9_3

[31] Singh, P., Tiwari, C. and Saxena, A. (2016) Variations in Solar Cycles 22, 23 & 24 and Their Effect on Earth's Climate. *International Journal of Astronomy and Astrophysics*, **6**, 8-13. https://doi.org/10.4236/ijaa.2016.61002